Flexible Collision-free Platooning Method for Unmanned Surface Vehicle with Experimental Validations

Du, B.; Lin, Bin; Xie, Wei; Zhang, Weidong; Negenborn, R. R.; Pang, Y.

DOI
10.1109/IROS47612.2022.9981043

Publication date
2022

Document Version
Final published version

Published in
Proceedings 2022 IEEE/RSJ International Conference on Intelligent Robots and Systems (IROS)

2022 IEEE/RSJ International Conference on Intelligent Robots and Systems (IROS)
October 23-27, 2022, Kyoto, Japan

Flexible Collision-free Platooning Method for Unmanned Surface Vehicle with Experimental Validations

Bin Du[1,2,4], Bin Lin[1,3], Wei Xie[1,2], Weidong Zhang[1,3], Rudy R. Negenborn[4], Yusong Pang[4]

Abstract— **This paper addresses the flexible formation problem for unmanned surface vehicles in the presence of obstacles. Building upon the leader-follower formation scheme, a hybrid line-of-sight based flexible platooning method is proposed for follower vehicle to keep tracking the leader ship. A fusion artificial potential field collision avoidance approach is tailored to generate optimal collision-free trajectories for the vehicle to track. To steer the vehicle towards and stay within the neighborhood of the generated collision-free trajectory, a nonlinear model predictive controller is designed. Experimental results are presented to validate the efficiency of proposed method, showing that the unmanned surface vehicle is able to track the leader ship without colliding with the surrounded static obstacles in the considered experiments.**

I. INTRODUCTION

In recent years, unmanned surface vehicle (USV) has been applied in many fileds, e.g., search and rescue, water quality monitoring, platooning transportation, etc., to name a few [1]. Due to the limited transportation capacity of a single ship, multi-vessel formation transportation could be the future alternative solution. A fleet of USVs with platooning could be used for the transportation in few of riverside cities [2] [3] [4]. However, platooning of USVs suffers from the risk of collision. Considering this problem, the aim of this work is to develop an platooning method for follower USV to follow a leader ship in an open environment without colliding with other vessels and obstacles.

The meaning of "platoon" is similar to the "formation", which can help to increase the vehicles' transport efficiency and reduce the cost [5]. Many results have been reported on USV platooning. The USV's behavior model based on navigational situations [6], [7], [8], was presented for path following, formation maintaining and obstacle avoidance within ports. The distributed flocking theoretical framework for distributed system was developed in [9], which controlled agents at uniform speeds while avoiding collisions. Economic assessment about application of USV platooning in the inland sector was studied in [10]. The choices of different types platooning in various scenarios were discussed in [11]. However, conventional method of platooning always requires followers to strictly follow the leader's movement route. As the position of the obstacle changes in real time, the follower USV should choose a flexible platooning route independently to track the leader ship without collisions.

It is still challenging for USV platooning designing collision avoidance method and putting it into application. Several attempts have been made to automate the collision avoidance. To obtain collision free paths, a monte-carlo sampling path planning method was developed in [12] for USV based on the monte-carlo and A* algorithm. In [13], a dynamic reciprocal velocity obstacles avoidance method was proposed for USVs to deal with the uncertainty of future behavior for obstacles avoidance. In [14], a robust distributed obstacle avoidance was developed for USV platooning by surrounding obstacles with stable cycles. Some platooning methods changed formation to follow the paths around static and dynamic obstacles. In [15] [16], model predict control (MPC) approaches were applied to calculate the optimal control inputs to achieve collision avoidance. The artificial potential field (APF) method was initially reported in [17] , whose basic idea was to build a virtual artificial potential field. We defined various potential functions that generate different forces, such as potential of leader ship generates attractive force for the follower USV and potential of obstacle generates repulsive forces, respectively. Then the gradient descent method was used to find the direction of gradient descent. Finally, a collision-free optimal platooning trajectory was obtained. However, in the conventional APF, the potential field has a saddle point, e.g., the follower USV, leader ship and obstacle are in a line, where the attractive force is equal to the repulsive force. This saddle point will cause the stagnation to the follower USV, that is the inherent drawback of conventional APF. To overcome this drawback, we develop a fusion artificial potential field (FAPF) method in which both virtual and tangential repulsion potential fields are introduced to reduce the local stagnation situations.

The main contributions of this paper are given as follows: In previous studies, the follower vessels in platooning strictly followed the trajectory of the leader ship, but when the obstacles changed their positions, the follower vessels had

This work is supported in part by the Hainan Province Science and Technology Special Fund under Grant ZDYF2021GXJS041, in part by the Key R&D Program of Guangdong under Grant 2020B1111010002, in part by the National Natural Science Foundation of China under Grant U2141234, in part by the Shanghai Science and Technology program under Grant 19510745200, in part by the Shanghai Sailing Program under Grant 22YF1420400, in part by the Stable Supporting Fund of Science and Technology on Underwater Vehicle Technology under Grant JCKYS2021SXJQR-01, in part by the European Union and the European Regional Development Fund, as part of the Interreg North Sea Region project AVATAR, and in part by the China Scholarship Council under Grant 202106230194.

[1]Department of Automation, Shanghai Jiao Tong University, Shanghai, 200240, China. {bin_du, fjpt-linbin, weixie, wdzhang}@sjtu.edu.cn

[2]National Key Laboratory of Science and Technology on Underwater Vehicle, Harbin Engineering University, Harbin, China.

[3]School of Information and Communication Engineering, Hainan University, Haikou, Hainan, China.

[4]Department of Maritime and Transport Technology, Delft University of Technology, Delft, Netherlands. {r.r.negenborn, Y.Pang}@tudelft.nl

2022 IEEE/RSJ International Conference on Intelligent Robots and Systems (IROS) | 978-1-6654-7927-1/22/$31.00 ©2022 IEEE | DOI: 10.1109/IROS47612.2022.9981043

the risk of collision. Therefore, we propose a flexible USV platooning method, which consists of three parts: First, a hybrid line-of-sigh (HLOS) based flexible platooning method is proposed for follower USV to automatically track leader ship. Second, a FAPF method is developed to generate a collision-free trajectory which can be directly navigated USV bypass obstacles. Finally, an online nonlinear model predictive controller (NMPC) scheme is developed with full state integration for stable and accurate tracking

II. USV'S KINEMATIC AND DYNAMIC MODEL

The USV is modeled as a rigid body regard to thrust and torque. An inertial coordinate frame $\{\boldsymbol{I}\}$ and a body-fixed coordinate frame $\{\boldsymbol{B}\}$ are introduced in this section. which are used for analyzing the motion of the vehicle. According to the mathematical model in [18], the kinematic of the follower USV are as follows:

$$\dot{\boldsymbol{\eta}} = \boldsymbol{J}(\psi)\boldsymbol{\nu}. \tag{1}$$

where $\boldsymbol{\eta} = [x, y, \psi]^\top$ and $\boldsymbol{\nu} = [u, v, \gamma]^\top$. The x and y are the coordinates of the vehicle's center of mass, and the ψ stands for the yaw angle. The $\boldsymbol{\nu}$ is the velocity vector including u, v and γ. The u and v denote the surge and the sway velocities, respectively. The γ indicates the yaw angular velocity. The matrix $\boldsymbol{J}(\psi)$ is the rotation matrix from $\{\boldsymbol{B}\}$ to $\{\boldsymbol{I}\}$ as shown below

$$\boldsymbol{J}(\psi) = \begin{bmatrix} \cos(\psi) & -\sin(\psi) & 0 \\ \sin(\psi) & \cos(\psi) & 0 \\ 0 & 0 & 1 \end{bmatrix}. \tag{2}$$

The dynamic model of USV is given below [18]:

$$\boldsymbol{M}\dot{\boldsymbol{\nu}} + \boldsymbol{O}(\boldsymbol{\nu})\boldsymbol{\nu} + \boldsymbol{F}(\boldsymbol{\nu})\boldsymbol{\nu} = \boldsymbol{\tau}_w + \boldsymbol{\tau}. \tag{3}$$

The $\boldsymbol{\tau}_w = [\tau_{wu}, \tau_{wv}, \tau_{w\gamma}]^\top$ stands for disturbances in surge, sway and yaw directions. The decoupled symmetric mass matrix $\boldsymbol{M}$ is described as:

$$\boldsymbol{M} = \mathrm{diag}\{m_{11}, m_{22}, m_{33}\}. \tag{4}$$

where m_{11},m_{22} and m_{33} are mass parameters [19]. The coriolis and centripetal matrix $\boldsymbol{O}(\boldsymbol{\nu})$ is given as:

$$\boldsymbol{O}(\boldsymbol{\nu}) = \begin{bmatrix} 0 & 0 & -m_{22}v \\ 0 & 0 & m_{11}u \\ m_{22}v & -m_{11}u & 0 \end{bmatrix}. \tag{5}$$

The damping matrix $\boldsymbol{F}(\boldsymbol{\nu})$ can be expressed as:

$$\boldsymbol{F}(\boldsymbol{\nu}) = \mathrm{diag}\{X_u, Y_v, N_r\}. \tag{6}$$

where X_u, Y_v, N_r are hydrodynamic coefficients.

Assumption 1: The hydrodynamic coefficients X_u, Y_v, and N_r are positive, constant, unknown, and satisfy [20]

$$|X_u| \le S_1, \quad |Y_v| \le S_2, \quad |N_r| \le S_3. \tag{7}$$

where S_1, S_2, S_3 are a positive number.

Assumption 2: The external disturbances are unknown, and satisfy [20]

$$\|\boldsymbol{\tau}_w\| \le B. \tag{8}$$

where B is a positive number. The disturbances formulated by external environment are formulated based on the randomness statistical analysis [21], [22].

The $\boldsymbol{\tau} = [\tau_u, \tau_v, \tau_\gamma]^\top$ denotes the thrust forces and torque, respectively.

$$\dot{\mathbf{p}}(t) = f(\mathbf{p}(t), \mathbf{u}(t)). \tag{9}$$

where $\mathbf{p} = [\boldsymbol{\eta}^\top, \boldsymbol{\nu}^\top]^\top$ is the state vector of USV.

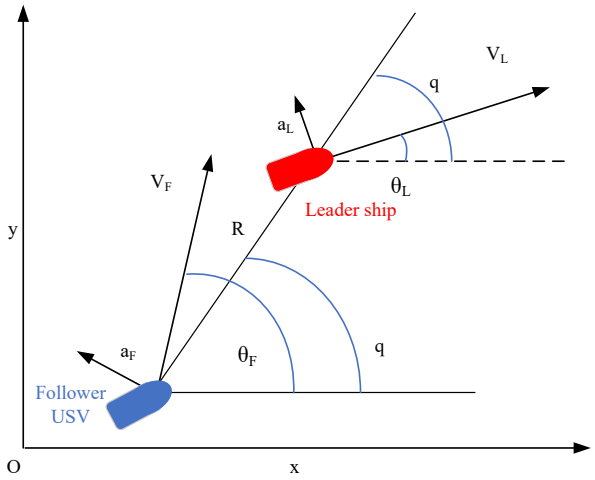

Fig. 1: The leader ship and follower USV's positions and velocities diagram.

III. HLOS BASED FLEXIBLE PLATOONING METHOD

In this paper, the leader ship is manned and follower USV is unmanned. We devise a platooning method for the follower USV to track the leader ship. The relationship between leader ship and follower USV are shown in Fig. 1. The kinematics equations [23] are expressed as:

$$\begin{aligned} \dot{R} &= V_L\cos(\theta_L - q) - V_F\cos(\theta_F - q). \\ \dot{q} &= R^{-1}\left[V_L\sin(\theta_L - q) - V_F\sin(\theta_F - q)\right]. \end{aligned} \tag{10}$$

where q and R are the follower USV's line-of-sight angle and the relative distance to the leader ship. V_F and V_L stand for the follower USV and the leader ship's velocities, θ_F and θ_L are the follower USV and the leader ship's heading angles. a_L and a_F are the accelerations of the leader ship and follower USV, respectively, that are counterclockwise perpendicular to their corresponding velocities. We have $\dot{\theta}_F = a_F {V_F}^{-1}$ and $\dot{\theta}_L = a_L {V_L}^{-1}$. The main work of platooning method is to design a guidance law providing reference heading angel θ_F^r, angular velocity $\dot{\theta}_F^r$ and velocity V_F^r for follower USV.

From Eq.(10), we have

$$V_F^r = \frac{V_L\cos(q - \theta_L) - \dot{R}}{\cos(\theta_F - q)}. \tag{11}$$

To make follower USV track leader ship in an optimal trajectory, we should design reference θ_F^r. In [24] [25], the proportional relationship between $\dot{\theta}_F^r$ and $\dot{q}$ was establish for aircraft approaching the target. Inspiriting from that work, a HLOS based platooning method is constructed by correlating $\dot{\theta}_F^r$ with the proportional, differential and integral terms of line-of-sight $\dot{q}$ as shown in Eq.(12).

$$\dot{\theta}_F^r = k_1\dot{q} + k_2\ddot{q} + k_3\int_{t_0}^{t_{tf}} \dot{q}dt. \tag{12}$$

After the integral term is simplified, Eq.(12) is rewritten as

$$\dot{\theta}_F^r = k_1\dot{q} + k_2\ddot{q} + k_3{t_{go}}^{-1}\left(q - q_0\right). \tag{13}$$

We have

$$\theta_F^r = \int_{t_0}^{t_{tf}} k_1\dot{q} + k_2\ddot{q} + k_3{t_{go}}^{-1}\left(q - q_0\right)dt. \tag{14}$$

where $k_1 = 5, k_2 = 3, k_3 = 1$. t_{go} is completion time of formation that can be defined as [23]

$$t_{\mathrm{go}} = \frac{R}{V_L}\left(1 + \frac{{\theta_L}^2}{2(2k_1 - 1)}\right). \tag{15}$$

The derivatives of Eq.(10) is

$$\ddot{q} = -R^{-1}\left[2\dot{R}\dot{q} - a_L\cos\left(q - \theta_L\right) + a_F\cos\left(q - \theta_F\right) + \dot{V}_F\sin\left(\theta_F - q\right)\right]. \tag{16}$$

Since a_L of the leader ship is unknown for the follower USV, a_L can be treated as an uncertainty. As the ship's acceleration should be continuous and bounded, we can refer to the mathematical model in [26] to describe the uncertain variable a_L.

$$\left|\frac{d^j a_L}{dt^j}\right| \leq \mu \quad \text{for } j = 0, 1, 2, \ldots, n. \tag{17}$$

Eq.(10) can be expressed as

$$\frac{d(R\dot{q})}{dt} = -\dot{R}\dot{q} + a_L cos\left(q - \theta_L\right) - a_F\cos\left(q - \theta_F\right) - \dot{V}_F\sin\left(\theta_F - q\right). \tag{18}$$

Form [27] and [28], the disturbance observer for $\hat{a}_L$ and $\dot{\hat{a}}_L$ can be defined as

$$\begin{cases} \hat{a}_L\cos\left(q - \theta_L\right) = p_{11} + l_{11}x_1 \\ \dot{p}_{11} = -l_{11}\left(x_2 + p_{11} + l_{11}x_1\right) + p_{12} + l_{12}x_1 \\ \dot{p}_{12} = -l_{12}\left(x_2 + p_{12} + l_{12}x_1\right) \end{cases} \tag{19}$$

where $x_1 = R\dot{q}$ and $x_2 = -\dot{R}\dot{q} - a_F\cos\left(q - \theta_F\right) - \dot{V}_F\sin\left(\theta_F - q\right)$ [27]. p_{11} and p_{12} are auxiliary variables. l_{11} and l_{12} are positive constants.

IV. FAPF OBSTACLE AVOIDANCE METHOD

The APF method has the characteristics of simple form, high precision and easy application [17]. To address the saddle point in the traditional APF, we developed a FAPF method for follower USV collision avoidance. In FAPF, the total potential is described as follow:

$$U(X) = U_a(X) + U_r(X). \tag{20}$$

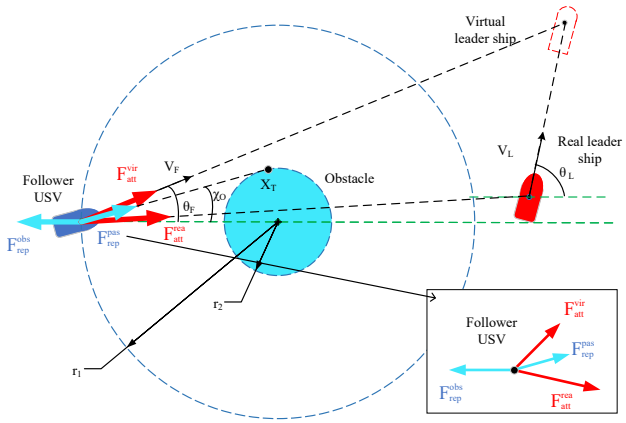

Fig. 2: The force diagram of follower USV in FAPF field.

To overcome the stagnation caused by the saddle point, we introduce the concept of virtual leader ship which provides additional potential with regard to the direction of motion of the leader ship. The position of the virtual leader ship is at the intersection of the heading of the real leader ship and the heading of the follower USV. In Eq.(20), the attractive potential function $U_a(X)$ is affected by both the real leader ship potential $U_a^r(X)$ and virtual leader ship potential $U_a^v(X)$.

$$U_a(X) = U_a^r(X) + U_a^v(X). \tag{21}$$

The $U_a^r(X)$ is related to the distance between the follower USV and the leader ship. The $U_a^v(X)$ is produced by the virtual leader ship.

$$\begin{cases} U_a^r(X) = \eta_a^r\left|X_F(t) - X_L^r(t)\right|^m \\ U_a^v(X) = \eta_a^v\left|X_F(t) - X_L^v(t)\right|^m. \end{cases} \tag{22}$$

$X_L^r(t)$, X_L^v and $X_F(t)$ represent the positions of the real leader ship, positions of the virtual leader ship and positions of the follower USV at time t, respectively. η_a^r, η_a^v and m are constants.

$$F_a(X) = -\nabla U_a(X). \tag{23}$$

The potential field formed by the obstacle will repel the follower USV. As the distance between follower USV and the obstacle decreases, the effect of the repulsive force increases. We add an extra component to repulsive potential that provides force along the obstacle's tangent direction (Fig. 2).

$$U_r^o(X) = \begin{cases} \frac{1}{2}\eta_r^o\left[\frac{1}{d} - \frac{1}{r_1}\right]^2, & d \leqslant r_1 \\ 0, & d > r_1 \end{cases} \tag{24}$$

$$U_r^p(X) = \begin{cases} \frac{1}{2}\eta_r^p\left[\frac{1}{d_T} - \frac{1}{r_1}\right]^2, & d \leqslant r_1 \\ 0, & d > r_1 \end{cases} \tag{25}$$

where $d = |X_F(t) - X_O|$ which is the distance between the follower USV and obstacle. $d_T = |X_F(t) - X_T|$ is the

distance between the follower USV and tangent point.

$$F_r(X) = -\nabla U_r(X). \tag{26}$$

The resultant force provieded by FAPF on follower USV is shown as:

$$F = F_a(X) + F_r(X). \tag{27}$$

The tangent point $X_T(x_T, y_T)$ can be formulated as

$$\begin{cases} x_T = (x_O - \mu_l y_F + \mu_l^2 x_F + \mu_l y_O)(1+\mu_l^2)^{-1} \\ y_T = (y_F + \mu_l x_O + \mu_l^2 y_O - \mu_l x_F)(1+\mu_l^2)^{-1} \end{cases} \tag{28}$$

where x_O, x_T, y_O and y_T are shown in Fig. 2. The variable of μ_l can be written as [29]:

$$\mu_l = \frac{x_O y_O + x_F y_F - x_F y_O - x_O y_F \pm r_2 \lambda_l}{-r_2^2 + x_O^2 - 2x_O x_F + x_F^2}. \tag{29}$$

where λ_l can be formulated as:

$$\lambda_l = \|(x_F - x_O) + (y_F - y_O) - r_2\|. \tag{30}$$

V. NMPC TRAJECTORY TRACKING CONTROL

The typical NMPC problem can be described as follows:

$$\begin{aligned} &\dot{\mathbf{p}}(t) = f(\mathbf{p}(t), \mathbf{u}(t)), \mathbf{p}(0) = \mathbf{p}_0. \\ &\text{s.t.} \quad \mathbf{p}(t) \in \mathbb{X}, \quad \mathbf{u}(t) \in \mathbb{U}. \end{aligned} \tag{31}$$

where $\mathbb{X} \subseteq \mathbb{R}^m$ and $\mathbb{U} \subseteq \mathbb{R}^n$ define the allowable state and control set respectively. The solution is obtained from finite horizon optimal control problem.

$$\begin{aligned} \min_{u(z)} h(\mathbf{p}(t), u(t)) = \int_t^{t+T} l(\mathbf{p}(z), \mathbf{u}(z)) dz + \\ L(\mathbf{p}(t+T)). \end{aligned} \tag{32}$$

subject to

$$\dot{\mathbf{p}}(z) = f(\mathbf{p}(z), \mathbf{u}(z)), \mathbf{p}(0) = \mathbf{p}_0. \tag{33}$$

$$\mathbf{p}(z) \in \mathbb{X}, \mathbf{u}(z) \in \mathbb{U}, \forall z \in [t, t+T]. \tag{34}$$

$h(\mathbf{p}(t), u(t))$ stands for the objective function. $l(\mathbf{p}(t), \mathbf{u}(t))$ is the phase cost function and $L(\mathbf{p}(t))$ is terminal cost function. $l(\mathbf{p}(t), \mathbf{u}(t))$ is described as

$$l(\mathbf{p}(t), \mathbf{u}(t)) = ||\mathbf{p}(t) - \mathbf{p}^r(t)||_{W_l} + ||\mathbf{u}(t)||_{W_u}. \tag{35}$$

W_l and W_u are positive semi-definite weighing matrices. $\mathbf{p}^r(t) = [\boldsymbol{\eta}^{rT}, \boldsymbol{\nu}^{rT}]^\top$ is the reference states in which $\boldsymbol{\eta}^r = [x_d, y_d, \psi_d]^\top, \boldsymbol{\nu}^r = [u_d, v_d, \gamma_d]^\top$. $L(\mathbf{p}(t))$ can be expressed as

$$L(\mathbf{p}_{t+T}) = ||\mathbf{p}(t+T) - \mathbf{p}^r(t+T)||_{W_L}. \tag{36}$$

W_L is the penalty matrix influencing the stability of the control. Final solutions are obtained from optimal control law: $\mathbf{u} = \mathbf{u}^*(\cdot, \mathbf{p}(t))$ which can be obtained by using infinite prediction and control horizons.

$$\dot{\mathbf{p}}(t) = f\left(\mathbf{p}(t), \mathbf{u} = \mathbf{u}^*(\cdot, \mathbf{p}(t))\right). \tag{37}$$

This optimal problem solved by Fmincon Sequential Quadratic Programming (FSQP) algorithm. According to the NMPC algorithm, the optimal control problem of real-time accurate trajectory tracking is effectively solved for the follower USV.

TABLE I: The basic parameters of USV.

Items	Characteristics
Size	2m×1.19m×0.75m
Maximum displacement	120kg
Draft of the ship	15cm
Thrusters	2 × 1.5kw brushless DC motor
Power energy	3 × 120Ah ternary lithium-ion batteries
Cruising time	4-5 hours
Maximum velocity	2m/s
Onboard sensors	RTK GPS, millimeter-wave radar

VI. EXPERIMENTS AND RESULTS

A. Experimental setup

We have developed an aluminum hull USV with dual propellers for optimal maneuverability, of which two sealed hollow shells at the bottom provide buoyancy for the hull. A hollow quadrilateral aluminum box with equipment is connected to two aluminum pontoons. The maximum displacement of the aluminum catamaran is 120kg and the maximum velocity is 2m/s. The detailed specifications are shown in Table.I.

The onboard computer on the USV runs Robot Operating System (ROS) as a middle-ware. It was responsible for sending its sensory values to the central computer, where the high-level computations, such as collision avoidance and path planning, were performed in Matlab. The SP70C millimeter-wave radar is the primary perception sensor to detect obstacles. The SP70C is a K-band radar sensor developed by the NANO radar company, which utilizes a 24GHz band and detects multi-targets(at most 8). It can measure the direction, range, velocity and angle of moving targets. The real-time kinematic positioning (RTK) GPS receivers are integrated on the bow and stern of USV. Two GPS receivers provide sub-meter position and linear accelerations for the USV. Two 25v × 1.5kw lithium batteries are installed in the quadrangular cabin. Our USV can cruise continuously for 4-5 hours on the calm water.

An accurate dynamic model of USV is essential for NMPC to achieve precise control. Since the established USV's dynamic model is an unknown model with undefined hydrodynamic parameters, such as m_{11}, m_{22}, m_{33}, X_u, Y_v, and N_r, all of parameters should be determined. The identification can be expressed as an optimization problem in (38) [2] [3]:

$$\begin{aligned} &\arg\min_{\kappa} \sum_t \varepsilon(t)^\top W \varepsilon(t). \\ &\text{s.t. } \kappa_l \leq \kappa \leq \kappa_u. \end{aligned} \tag{38}$$

where $\kappa = [m_{11}, m_{22}, m_{33}, X_u, Y_v, N_r]^\top$, κ_l and κ_u are the lower and upper bounds of κ. $W \in \mathbb{R}^{3\times3}$ stands for the weight matrix for the optimization. $\varepsilon(t)$ donates the error from the real experiment. After experiment and measurement, we get identified hydrodynamic parameters $m_{11} = 115.50, m_{22} = 180.69, m_{33} = 73.61, X_u = 61.36, Y_v = 180, N_r = 123.08$.

The experiment was conducted as follows. First, we arranged moored vessels are distributed along the river as static

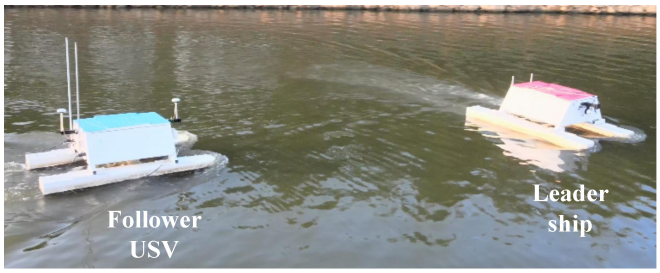

(a)

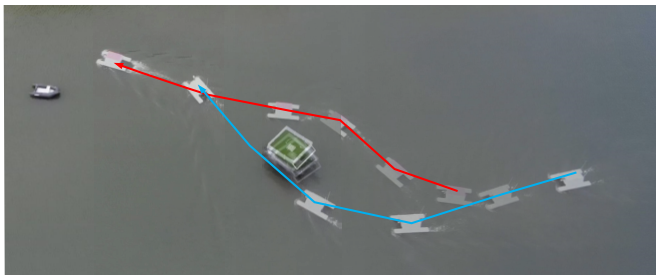

(b)

Fig. 3: (a) The Leader ship and follower USV. (b) The display of USV flexible platooning with obstacle.

obstacles. Then, we organized one remote controlled leader ship and one autonomous follower USV in the river. After setting up the shore-based communication equipment, we assigned state information of leader ship for the follower USV. The HLOS based platooning method will generate a feasible V_F^r, θ_F^r and $\dot{\theta}_F^r$ for the follower USV. When the obstacles would block the follower USV approach the leader ship, the collision avoidance method based on PFAP created a collision-free route for the follower USV. Lastly, the follower USV starts to track the reference trajectories by NMPC method to form a platooning. We experimented with straight platooning and circle platooning respectively. Both field tests were performed on Huchuntang River in Shanghai, China. We repeated the each tests several times during the experiments.

B. Main results

Fig. 3 displays a experimental scenario and we dissect it to explain the autonomy process. The follower USV executed both tracking and collision avoidance manoeuvres between two moored vessels. At first, the follower USV tracks the leader ship, their trajectories are shown as blue and red line respectively. The follower USV detects the obstacle on the way and generates optimal collision avoidance route. After obstacle avoidance, the follower USV re-tracks the leader ship and returns to the platooning path.

The results of straight platooning are shown in Fig. 4 and Fig. 5. In Fig. 4, as the follower USV tries to approach the leader ship from start point, it is forced to track leader ship while going to the right of moored vessel. The obstacle forces the USV coming cross from right direction. Before the second obstacle, the obstacle avoidance path of the follower USV depends on the direction of movement of the leader ship. In Fig. 5(a), the black circle depicts impassable obstacles. The trajectories of follower USV and leader ship are shown in blue and red respectively. Fig. 5(b) reflects the change process of the heading angle of both the follower USV and the leader ship. The speed changes of the two ships are shown in Fig. 5(c). The follower USV successfully avoided all obstacles in the experiments. The guidance, collision avoidance and control methods are validated by this experiment.

Fig. 6 depicts the experiment results of circle platooning. We can see that even leader ship does a circular motion around the center of obstacle, the trajectory of follower USV is stable and collision-free. All of experiments in Fig. 4(a)(b) and Fig. 6 have been repeatedly tested. Results of experiment shows that the follower USV can complete platooning around obstacles. These extensive experiments demonstrate the effectiveness of our autonomy system for river waterways. Our proposed method could successfully control the follower USV being along with the leader ship without collision.

VII. CONCLUSIONS

In a multi-ship platooning, the follower USV should flexibly plan a route based on the surrounding environment. This paper proposed a flexible platooning method to generate a collision-free trajectory for follower USV. To achieve this purpose, we present HLOS based flexible platooning method for USV and it can flexibly select the optimal movement trajectory according to the environment. An integrated collision avoidance is achieved by the FAPF method in which both virtual and tangential repulsion potential fields are introduced to reduce the local stagnation situations. We formulated a NMPC method for the follower catamaran vessel to track the optimal trajectory. Finally, we developed a aluminum catamaran USV that can perform guidance, collision avoidance and accurate tracking control in the river waterways in the scope of the experiments considered. Experimental results have validated the efficiency of proposed flexible platooning method in straight and circle platooning scenarios, which is critical for accomplishing advanced autonomous missions, e.g., cooperative platooning of distributed USVs for unmanned transportation.

REFERENCES

[1] R. Yan, S. Pang, H.-b. Sun, and Y. Pang, "Development and missions of unmanned surface vehicle," *Journal of Marine Science and Application*, vol. 9, no. 4, pp. 451–457, 2010.

[2] W. Wang, L. A. Mateos, S. Park, P. Leoni, B. Gheneti, F. Duarte, C. Ratti, and D. Rus, "Design, modeling, and nonlinear model predictive tracking control of a novel autonomous surface vehicle," in *2018 IEEE International Conference on Robotics and Automation (ICRA)*, pp. 6189–6196, IEEE, 2018.

[3] W. Wang, B. Gheneti, L. A. Mateos, F. Duarte, C. Ratti, and D. Rus, "Roboat: An autonomous surface vehicle for urban waterways," in *2019 IEEE/RSJ International Conference on Intelligent Robots and Systems (IROS)*, pp. 6340–6347, IEEE, 2019.

[4] W. Wang, T. Shan, P. Leoni, D. Fernández-Gutiérrez, D. Meyers, C. Ratti, and D. Rus, "Roboat ii: A novel autonomous surface vessel for urban environments," in *2020 IEEE/RSJ International Conference on Intelligent Robots and Systems (IROS)*, pp. 1740–1747, IEEE, 2020.

(a)

(b)

Fig. 4: The experiment of straight platooning with different routes based on the time-line. (a) Route 1 (b) route 2.

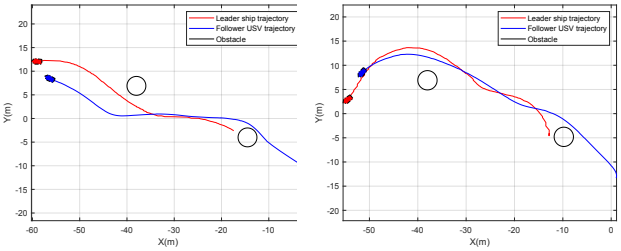

(a)

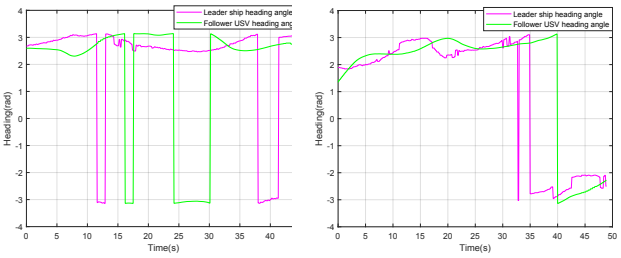

(b)

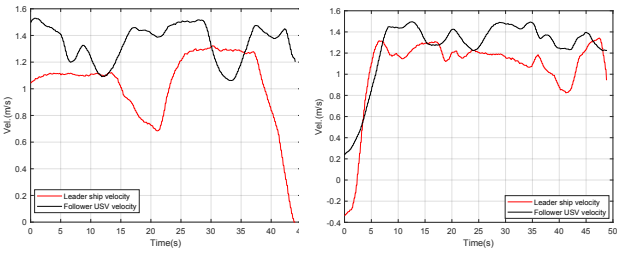

(c)

Fig. 5: The performance of straight platooning with different routes. (a) Trajectories (b) heading angles (d) velocities.

[5] A. Colling, R. Hekkenberg, and E. van Hassel, "A viability study of waterborne platooning on the lower rhine," *European Journal of Transport and Infrastructure Research*, vol. 21, pp. 71–94, 5 2021.

[6] L. Chen, R. R. Negenborn, and H. Hopman, "Intersection crossing of cooperative multi-vessel systems," *IFAC-PapersOnLine*, vol. 51, no. 9, pp. 379–385, 2018.

[7] L. Chen, A. Haseltalab, V. Garofano, and R. R. Negenborn, "Eco-vtf: Fuel-efficient vessel train formations for all-electric autonomous ships," in *2019 18th European Control Conference (ECC)*, pp. 2543–2550, IEEE, 2019.

[8] L. Chen, Y. Huang, H. Zheng, H. Hopman, and R. Negenborn, "Cooperative multi-vessel systems in urban waterway networks," *IEEE Transactions on Intelligent Transportation Systems*, vol. 21, no. 8, pp. 3294–3307, 2019.

[9] R. Olfati-Saber, "Flocking for multi-agent dynamic systems: Algorithms and theory," *IEEE Transactions on automatic control*, vol. 51, no. 3, pp. 401–420, 2006.

[10] H. Meersman, E. Moschouli, L. NanwayBoukani, C. Sys, E. van Hassel, T. Vanelslander, and E. Van de Voorde, "Evaluating the performance of the vessel train concept," *European Transport Research Review*, vol. 12, no. 1, pp. 1–11, 2020.

[11] A. P. Colling and R. G. Hekkenberg, "A multi-scenario simulation transport model to assess the economics of semi-autonomous platooning concepts," *COMPIT 2019*, pp. 132–145, 2019.

[12] P. Agrawal and J. M. Dolan, "Colregs-compliant target following for an unmanned surface vehicle in dynamic environments," in *2015 IEEE/RSJ International Conference on Intelligent Robots and Systems (IROS)*, pp. 1065–1070, IEEE, 2015.

[13] D. K. M. Kufoalor, E. F. Brekke, and T. A. Johansen, "Proactive collision avoidance for asvs using a dynamic reciprocal velocity obstacles method," in *2018 IEEE/RSJ International Conference on Intelligent Robots and Systems (IROS)*, pp. 2402–2409, IEEE, 2018.

[14] B. Wang, S. G. Nersesov, and H. Ashrafiuon, "Robust formation control and obstacle avoidance for heterogeneous underactuated surface vessel networks," *IEEE Transactions on Control of Network Systems*, vol. 9, no. 1, pp. 125–137, 2022.

[15] Z. Du, V. Reppa, and R. R. Negenborn, "Mpc-based colregs compliant collision avoidance for a multi-vessel ship-towing system," in *2021 European Control Conference (ECC)*, pp. 1857–1862, IEEE, 2021.

[16] M. van Pampus, A. Haseltalab, V. Garofano, V. Reppa, Y. Deinema, and R. R. Negenborn, "Distributed leader-follower formation control for autonomous vessels based on model predictive control," in *2021 European Control Conference (ECC)*, pp. 2380–2387, IEEE, 2021.

[17] O. Khatib, "Real-time obstacle avoidance for manipulators and mobile robots," in *Autonomous robot vehicles*, pp. 396–404, Springer, 1986.

[18] B. Du, B. Lin, C. Zhang, B. Dong, and W. Zhang, "Safe deep reinforcement learning-based adaptive control for usv interception mission," *Ocean Engineering*, vol. 246, p. 110477, 2022.

[19] T. I. Fossen, "Handbook of marine craft hydrodynamics and motion control," in *John Wiley & Sons*, 2011.

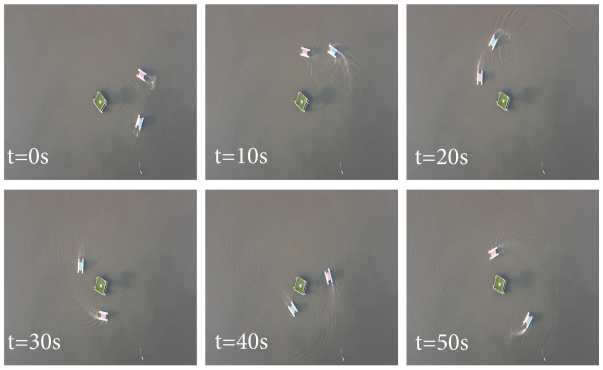

(a)

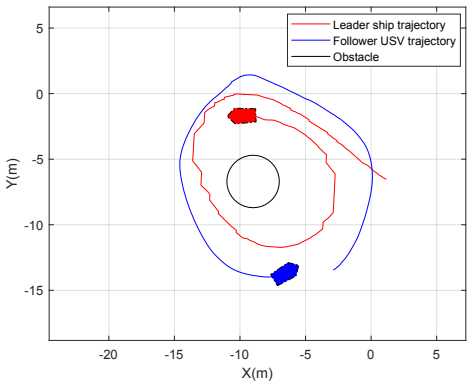

(b)

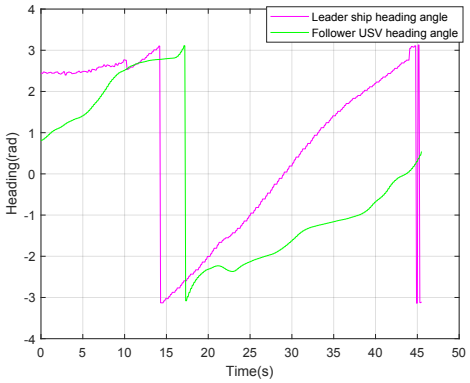

(c)

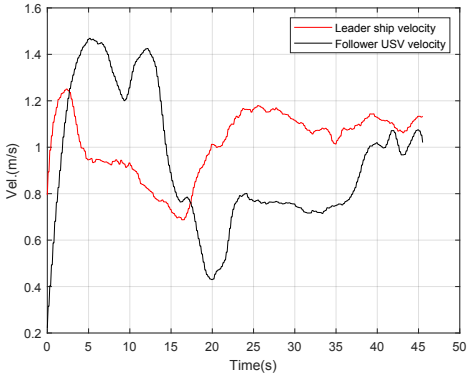

(d)

Fig. 6: The experiment of circle platooning. (a) Top view (b) Trajectories (c) heading angles (d) velocities.

[20] W. Xie, D. Cabecinhas, R. Cunha, and C. Silvestre, "Robust motion control of an underactuated hovercraft," *IEEE Transactions on Control Systems Technology*, vol. 27, no. 5, pp. 2195–2208, 2018.

[21] Y. Zhao, X. Qi, Y. Ma, Z. Li, R. Malekian, and M. A. Sotelo, "Path following optimization for an underactuated usv using smoothly-convergent deep reinforcement learning," *IEEE Transactions on Intelligent Transportation Systems*, vol. 22, no. 10, pp. 6208–6220, 2020.

[22] Z. Peng, D. Wang, Z. Chen, X. Hu, and W. Lan, "Adaptive dynamic surface control for formations of autonomous surface vehicles with uncertain dynamics," *IEEE Transactions on Control Systems Technology*, vol. 21, no. 2, pp. 513–520, 2012.

[23] B. Du, Y. Lu, X. Cheng, W. Zhang, and X. Zou, "The object-oriented dynamic task assignment for unmanned surface vessels," *Engineering Applications of Artificial Intelligence*, vol. 106, p. 104476, 2021.

[24] M. Golestani and I. Mohammadzaman, "Pid guidance law design using short time stability approach," *Aerospace Science and Technology*, vol. 43, pp. 71–76, 2015.

[25] G. M. Siouris, "Missile guidance and control systems," in *Springer Science & Business Media*, 2004.

[26] S. He, D. Lin, and J. Wang, "Robust terminal angle constraint guidance law with autopilot lag for intercepting maneuvering targets," *Nonlinear Dynamics*, vol. 81, no. 1, pp. 881–892, 2015.

[27] S. Lyu, X. Yan, and S. Tang, "Prescribed performance interceptor guidance with terminal line of sight angle constraint accounting for missile autopilot lag," *Aerospace Science and Technology*, vol. 69, pp. 171–180, 2017.

[28] D. Ginoya, P. Shendge, and S. Phadke, "Sliding mode control for mismatched uncertain systems using an extended disturbance observer," *IEEE Transactions on Industrial Electronics*, vol. 61, no. 4, pp. 1983–1992, 2013.

[29] D. Wang, P. Wang, X. Zhang, X. Guo, Y. Shu, and X. Tian, "An obstacle avoidance strategy for the wave glider based on the improved artificial potential field and collision prediction model," *Ocean Engineering*, vol. 206, p. 107356, 2020.